Available online at www.sciencedirect.com
SCIENCE DIRECT®
ELSEVIER
Journal of Photochemistry and Photobiology A: Chemistry 166 (2004) 149–154
Journal of Photochemistry and Photobiology A:Chemistry
www.elsevier.com/locate/jphotochem

Nanopatterning with conformable phase masks

Joana Maria [a], Seokwoo Jeon [a], John A. Rogers [a,b,*]

[a] *Department of Materials Science and Engineering, Frederick Seitz Materials Research Laboratory, Beckman Institute for Advanced Science and Technology, University of Illinois, Urbana/Champaign, 1304 West Green Street, Room 308, Urbana, IL 61801, USA*
[b] *Department of Chemistry, Frederick Seitz Materials Research Laboratory, Beckman Institute for Advanced Science and Technology, University of Illinois, Urbana/Champaign, 1304 West Green Street, Room 308, Urbana, IL 61801, USA*

Received 29 October 2003; received in revised form 13 February 2004; accepted 5 April 2004

Abstract

This paper describes an approach for using conventional photoresist materials to pattern structures with dimensions as small as 50 nm. This method, known as near field phase shift lithography (NFPSL), is an experimentally simple approach to nanofabrication that relies on ultraviolet exposure of a layer of resist while it is in conformal, atomic scale contact with such an elastomeric phase mask. This paper presents some representative structures produced with this method; it illustrates an example of its use in patterning the critical dimensions of organic transistors; and it outlines some new modeling results of the optics associated with this technique.
© 2004 Elsevier B.V. All rights reserved.

Keywords: Photolithography; Phase mask; Near field optics; Nanofabrication; Soft lithography; Elastomer

1. Introduction

The rapidly growing fields of nanoscience and nanotechnology have stimulated considerable interest in methods for building structures that have nanometer dimensions. In the past, research and development in this area has been driven mainly by the needs of the microelectronics industry. The spectacularly successful nanofabrication techniques that have emerged from those efforts—projection mode photolithography, electron beam lithography, etc.—are extremely well suited to the tasks for which they were principally designed: forming structures of radiation sensitive materials (e.g. photoresists or electron beam resists) on ultraflat glass or semiconductor surfaces. These approaches require sophisticated facilities, however, whose high cost makes them unavailable to large segments of the research community. As a result, there is interest in patterning techniques that offer nanometer resolution with experimentally simple setups. Considerable progress has been made in this area in the last few years, mainly by reexamining several of the conceptually oldest lithographic methods—molding, printing, embossing and writing [1,2]. This paper summarizes some of our past work on a simple type of high resolution photolithographic technique. The method, which we refer to as near field phase shift lithography (NFPSL) involves exposure of a photoresist layer to ultraviolet (UV) light that passes through an elastomeric phase mask while the mask is in conformal contact with the resist [3,4]. This approach requires only a phase mask and a handheld UV lamp to generate structures with dimensions as small as 50 nm over large areas (many cm^2, limited only by the size of the mask). The following presents several structures and devices that we have produced, and it summarizes a simple scalar theory that captures, in a semi-quantitative way, some aspects of the technique. It also describes some recent full vector finite element modeling of the optics. We explain how these new modeling efforts can explain certain subtle features of the technique and how they provide insights into extending the resolution and capabilities of the technique.

2. Experimental/materials and methods

Fig. 1(a) and (b) show schematic illustrations and images of the experimental approach and setup, respectively. The casting and curing procedures of soft lithography can generate high resolution phase masks out of the elastomer poly (dimethylsiloxane) (Sylgard 184, Dow Corning) [2]. These masks are transparent to UV light with wavelengths greater than 300 nm. Light passing through them is modulated in phase by an amount determined by the index of the PDMS (∼1.43) and the depth of the relief on the surface of the mask. This depth is equal to that on the 'master'

* Corresponding author. Tel.: +1-217-244-4979; fax: +1-217-244-1190.
E-mail address: jrogers@uiuc.edu (J.A. Rogers).

1010-6030/$ – see front matter © 2004 Elsevier B.V. All rights reserved.
doi:10.1016/j.jphotochem.2004.04.035

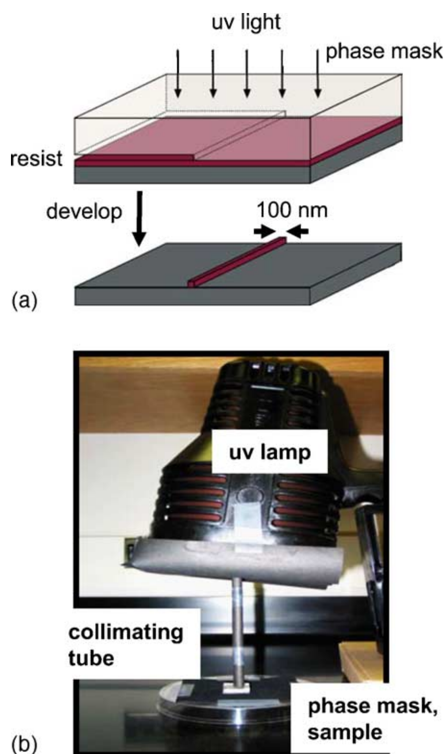

Fig. 1. (a) Schematic illustration of the photolithography process. Bringing an elastomeric phase mask into contact with a thin layer of photoresist causes the mask to 'wet' the surface of the resist. Passing ultraviolet light through the mask while it is in contact exposes the resist to the distribution of intensity that develops at the surface of the mask. For the case of a mask with a depth of relief that is designed to modulate the phase of the transmitted light by π a local null in the intensity appears at the step edge of relief. When a positive resist is used, exposure through such a mask followed by development yields a line of resist with a width equal to the characteristic width of the null in intensity. For 365 nm light and conventional photoresists, this width is approximately 100 nm. (b) Image of the experimental setup. An incoherent lamp and a tube for collimating its output provide light for the exposure.

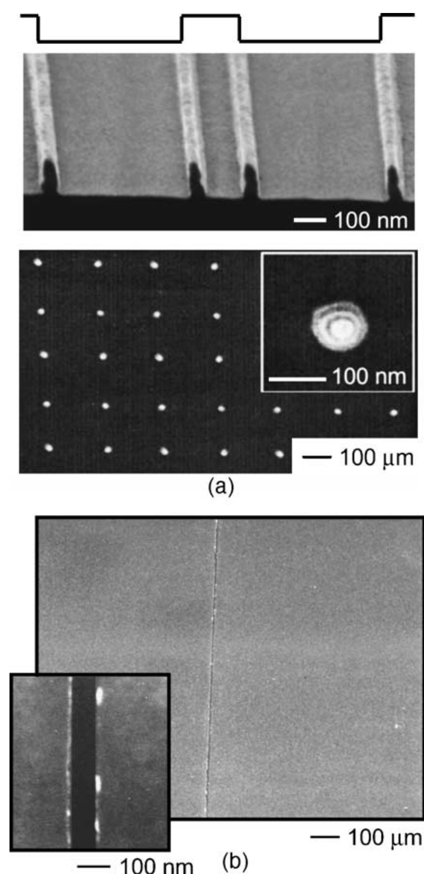

Fig. 2. (a) Scanning electron micrographs of typical structures in photoresist produced with the phase shifting photolithographic technique. The top frame shows lines with widths of ~50 nm. The lines above the image illustrate the positions of the relief features on the mask. Exposing the resist through this mask twice with a 90° rotation in between exposures produces arrays of dots of resist that have diameters of ~100 nm. (b) SEM of a pattern of Au formed by liftoff using line of resist similar to the one shown in part (a).

used to generate the mask. For the results shown here, the masters consisted of thin layers of resist (Shipley 1805) patterned by contact mode photolithography (Karl Suss MJB3 Mask Aligner) on silicon wafers [3,4]. The thicknesses of these layers (~400 nm for the experiments described here) were selected by controlling the speed of the spin casting (5000 rpm for 45 s) used to deposit them. This depth modulates the phase of transmitted 365 nm light (a strong emission line in mercury lamps) by an amount that is close to π. With this design, local minima in the intensity of transmitted light appear at the step edges of relief in the masks. By bringing such a mask into conformal, atomic scale contact with a layer of resist (this contact, which is driven mainly by van der Waals interactions, happens spontaneously without the application of pressure), and then passing UV light through the mask, it is possible to expose the resist to the distribution of intensity that exists at the surface of the mask [3]. Developing away the exposed regions of the resist (in the case that a positive resist is used) yields structures with geometries defined by the dark regions in the distribution of intensity near the mask. In principle, this technique represents a form of near field photolithography. It is important to note, however, that in many cases, the evanescent contribution to the intensity distribution at the surface of the mask is relatively small.

Fig. 1(b) displays an image of a simple experimental setup similar to the one used for these exposures. It consists of a conventional incoherent mercury lamp as a source of UV light. A tube provides a certain degree of geometrical collimation in the light used for exposure. The phase mask and photoresist are placed at the exit of the tube. Fig. 2 presents some scanning electron micrographs (SEMs) of structures produced with this type of apparatus [3–6]. The top frame in part (a) shows angled views of lines of photoresist that form at the edges of relief in the phase masks after exposure and development. (The relief structure of the mask is shown schematically at the top of this image.) Lines with complex curvilinear shapes are also possible. Multiple sequential ex-

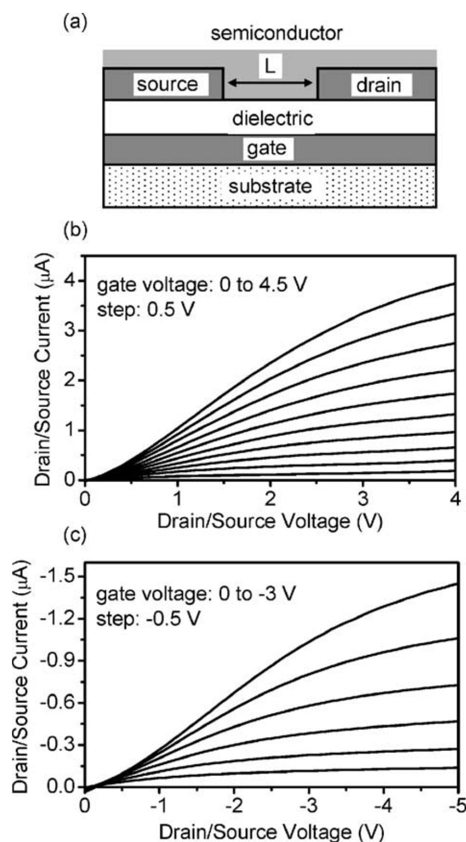

Fig. 3. (a) Schematic illustration of a thin film organic transistor. Phase shifting lithography with a conformable mask is well suited for generating very small separations between source and drain electrodes by liftoff. These electrodes can be used in organic transistors that have short channel lengths. (b) Current–voltage (IV) characteristics of an organic transistor with a 100 nm channel length formed using the technique described here. This transistor uses the organic semiconductor alphasexithiophene and behaves as a p channel device. (c) IV characteristics of a similar device that uses the n type organic semiconductor fluorinated copper pthalocyanine. The dielectric in both cases is a 20 nm layer of SiO_2.

posures provide additional flexibility in the geometries of patterns that can be produced. The bottom frame of Fig. 2(a) shows, as an example, arrays of 100 nm diameter posts of photoresist. These structures were produced by two exposures using a mask similar to the one illustrated in the top frame of Fig. 2(a) with a 90° rotation of the mask between exposures. These structures of resist can be used with conventional techniques to produce patterns in other materials, by etching, growth or liftoff. Fig. 2(b) shows a 100 nm wide slit in a thin film of Ti (1.5 nm)/Au (20 nm) on a silicon wafer, produced by first depositing Ti/Au onto a substrate that supports a line of photoresist similar to the ones shown in Fig. 2(a). Washing the resist away with acetone completes the fabrication.

Patterns of functional materials such as these can be incorporated into high performance devices. Fig. 3 illustrates, as an example, the use of structures of Ti/Au like the one shown in Fig. 2(b) for source/drain electrodes in thin film transistors that use organic semiconductors [6]. Here, thermally evaporating small molecule organic semiconductors onto prepatterned Ti/Au electrodes on thin films of SiO_2 (gate dielectric) on heavily doped silicon wafers (gate) completes the devices. Fig. 3(a) schematically shows their layout. The NFPSL procedures and liftoff procedures described above define the channel length; it is ∼100 nm for the devices whose current–voltage characteristics appear in Fig. 3(b) and (c). The on/off ratios are comparable to those observed in more conventional micron scale devices that use the same materials. The apparent mobilities extracted from these data are smaller, however, than those of the larger devices. We believe that the relatively small mobilities are related to the strong influence of contact resistances at these extremely small geometries.

3. Theory and calculation

Fig. 4 shows results of scalar computations of the distribution of intensity at the surface of a phase mask. The details of these calculations appear elsewhere [4,7]. Briefly, they approximate the phase mask by a two-dimensional transmission function that describes the geometry and phase depth of the features on the mask. This transmission function determines, by Fourier transformation, a diffraction pattern. Filtering this pattern to remove diffracted beams that emerge from the mask at angles greater than 90°, followed by recombining these beams at the surface of the mask defines the computed intensity distribution. All of the approximations associated with Fraunhofer diffraction are built into this analysis. The key results of the calculation are: (i) nulls in the intensity appear at the step edges of binary masks with relief depths that modulate the phase of the transmitted light by π;

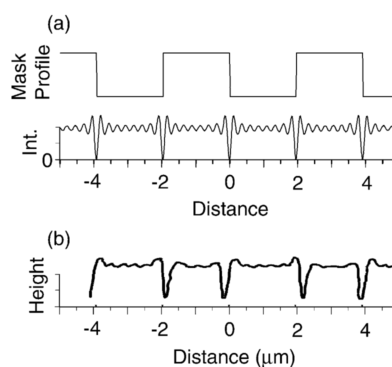

Fig. 4. (a) Intensity distribution at the surface of a phase mask, as computed using scalar diffraction theory. These results predict complete nulls in intensity at the step edges of relief when the phase is modulated by π. The widths of these dips in intensity are ∼100 nm when 365 nm is used with conventional resists. Not also the symmetric behavior of the intensity: the distribution under the raised regions of relief in the mask are the same as those under the recessed regions. (b) Relief profile in image reversal resist processed so that the height correlates linearly to the intensity at the surface of the mask. These measurements reveal some features that are different than those predicted by scalar theory.

(ii) the widths of the distributions of intensity around these nulls are ∼100 nm when 365 nm light is used with conventional photoresists (refractive indices between 1.6 and 1.7); and (iii) the intensity distributions involve small amplitude oscillations at locations between these nulls; these oscillations have the same amplitude and frequency in the recessed and raised regions of the mask (i.e. regions that do not and do contact the resist, respectively). Some of these features are observed experimentally. For example, the widths of the photoresist structures are 50–100 nm depending on the processing conditions and the mask design [8]; this range of feature sizes is qualitatively consistent with computed widths of ∼100 nm. Certain deviations from the simple model can be observed, however, through careful experiments that use image reversal photoresists to determine the intensity distribution near the surface of the mask. These measurements, which involve atomic force microscopy of the surface relief that develops on the resist after exposure and development (see Fig. 4(b)) reveal the intensity oscillations that are predicted by the scalar theory. They indicate, however, that these oscillations have different forms in the recessed and raised regions of the mask. In particular, the oscillations in the recessed regions have lower amplitude and spatial frequency than those in the raised regions. In addition, the patterns of resist show two other asymmetries: (i) the resist receives a higher dose in the raised regions than in the recessed regions and (ii) the developed lines of resist tend to show profiles that are skewed toward the recessed regions. Experiments also suggest that the intensity does not decrease completely to zero at the step edges. Although this effect could result from imperfect masks, it may also suggest deficiencies in the scalar calculations. In order to capture some of these experimentally observed aspects using the scalar model, we previously introduced mechanical sagging of the raised regions of the mask (which is known to occur in these low modulus PDMS materials for certain mask designs) and reflection losses associated with passage of light through the PDMS/air and air/resist interfaces for the recessed regions and through the PDMS/resist interface in the raised regions [7]. The reflection losses reduce the intensity by a larger amount in the recessed regions than in the raised regions. Mechanical sagging reduces the amplitude of the oscillations in these same regions, but neither effect alters their spatial frequencies.

Because of these and other deficiencies that arise from the approximations inherent to the scalar model, and because we believe that a better understanding of the detailed optics of the system will enable improvements in resolution, we performed full vector finite element modeling (FEM) of the system. We used a commercial FEM solver for this purpose (FEMLAB, Inc.). This approach discretizes the solution space of a system of partial differential equations and iteratively solves the problem at the nodes of the finite element mesh. The governing equations (i.e. Maxwell's equations) as applied to our system, which consists of a PDMS phase mask in the form of a binary grating of infinite spatial extent along the grating and perpendicular to it, in contact with a thick layer of photoresist are:

$$\nabla \times (\mu^{-1}\nabla \times \mathbf{E}) - \omega^2\varepsilon_c\mathbf{E} = 0,$$
$$\nabla \times ({\varepsilon_c}^{-1}\nabla \times \mathbf{H}) - \omega^2\mu\mathbf{H} = 0 \quad (1)$$

Here ε_c is the complex permittivity $\varepsilon_c = \varepsilon - j\sigma/\omega$. Even though the photoresist absorbs UV light, for simplicity we assume that it is completely transparent. Its permittivity as well as that of the PDMS and the air are real.

The relevant boundary conditions at interfaces between the different media are:

$$\mathbf{n}_2 \times (\mathbf{E}_1 - \mathbf{E}_2) = 0, \quad \mathbf{n}_2 \times (\mathbf{H}_1 - \mathbf{H}_2) = 0 \quad (2)$$

where we assume there are no surface currents. For boundaries representing a non-physical border (the top surface of the mask, the bottom surface of the resist) we use low-reflecting boundary conditions. We employ periodic boundary conditions at the lateral edges of our system to capture its infinite extent in this direction. The electric field has only one non-zero component, which can be chosen either perpendicular or parallel to the grating wavevector.

The code generates a finite element mesh using the Delaunay algorithm in order to ensure compatibility with the geometry, while still keeping the finite element angles as large as possible. The mesh can be controlled directly by adjusting the global element size of the mesh or the element size on an edge, domain, etc. In all cases we use a minimum of 8 mesh elements per wavelength. An iterative solver of the type GMRES, which is a Krylov subspace method is used to solve the mesh. GMRES is restarted every mth step and the convergence criterion is based on the residual. We use a pre-conditioner of the type Incomplete LU.

The numerical solution allows access to any physical quantity associated with the problem: electric field, magnetic field, electric energy, magnetic energy, total energy, phase angle, etc. Fig. 5 shows a plot of the total intensity for a system identical to the one illustrated in Fig. 4. These distributions are qualitatively similar to those determined by the scalar model in the sense that they predict nulls with characteristic widths of ∼100 nm and they show in-

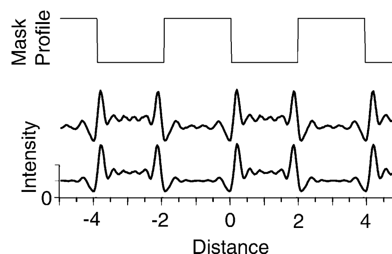

Fig. 5. Intensity distribution at the surface of a phase mask, as computed using full vector finite element modeling. The results predict slightly different behaviors for the TM and TE polarization states. They also show that incomplete nulls in intensity and different intensity distributions below the raised and recessed regions of the mask. All of these features are observed experimentally.

tensity oscillations. Unlike the scalar results, however, the FEM computations are also qualitatively consistent with the other experimental features discussed above. For example, the lower intensities as well as the lower amplitudes and frequencies of the oscillations in the recessed regions, compared to the raised regions, emerge naturally from the model (without including sagging in the recessed regions of the mask). Furthermore, the model shows an asymmetry in the shape of the dips in intensity, with distributions skewed slightly toward the recessed regions. The FEM results also show that the nulls in intensity predicted by the scalar model for an ideal π-shifting mask are not true nulls. The residual intensity that exists in these locations is consistent with the experimental ability to develop away all of the resist by leaving the sample in the developer for a time slightly longer than the optimum. (We note, however, that this experimentally observed effect could also be due simply to masks that do not shift the phase by exactly π and/or which have non-vertical sidewalls or other imperfections.) It is important to highlight, however, that the FEM results do not quantitatively account for the profiles shown in Fig. 4(b). We believe that the differences are due mostly to the combined effects of: (i) non-ideal features in the mask (e.g. depths that deviate from those required for π phase shifting and sloping sidewalls) and (ii) broadband, incoherent light that was used for the exposures compared to fully coherent, single wavelength light used in the FEM simulations. Future simulation and experimental work will investigate these effects further.

The ability of FEM modeling to capture nearly all of the important qualitative effects gives us confidence that it can be used to understand aspects of the system that have not yet been observed experimentally. Fig. 6(a) shows the computed depth evolution of the distribution of intensity. These results clearly illustrate that resolution is lost as light passes through the first several hundred nanometers of resist. Fig. 6(b) shows the depth evolution of the characteristic width of the dip in intensity that forms near edges of relief on the mask. This effect emphasizes not only the importance of the conformal contact between the mask and resist during exposure, but it also suggests that ultrathin resists may improve the resolution. Secondly, the results of Fig. 5 indicate that the local minima that develop when light polarized parallel to the grating passes through the mask are deeper (i.e. there is a larger degree of modulation) than those for perpendicular polarized light. Polarization control may, therefore, also improve the process. Thirdly, the complex three-dimensional (3D) distributions of intensity that appear at distances of many

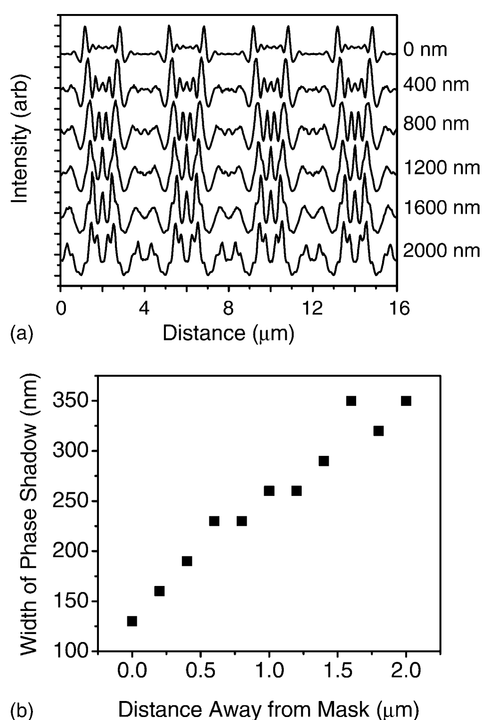

Fig. 6. (a) Intensity distribution computed with a full vector model at different distances away from the surface of a phase mask. The widths of the dips in intensity that occur at the phase mask edges increase with distance away from the phase mask; the spatial frequencies of the fluctuations in intensity near these nulls also decrease with depth. (b) Variation in the characteristic width of the dip in intensity that occurs at the edges of relief in the phase mask. This width increases with distance away from the mask.

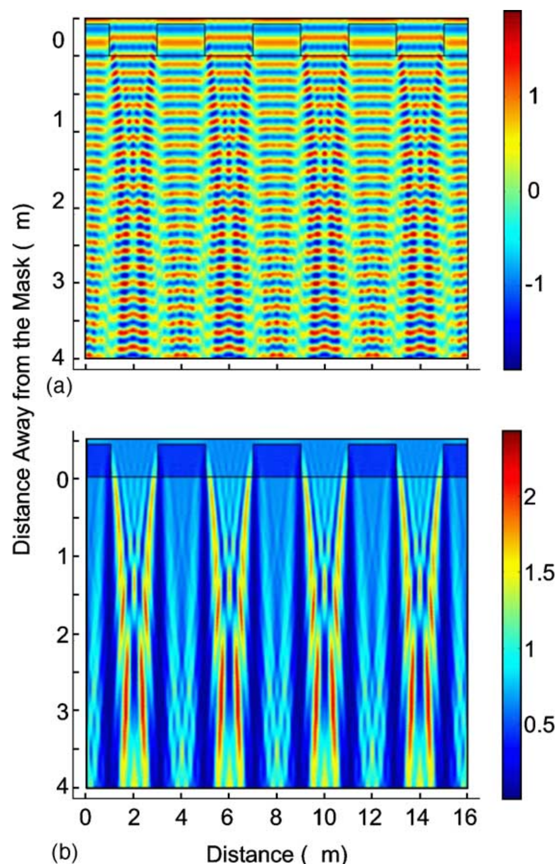

Fig. 7. (a) Electric field amplitude computed for a plane wave passing through a phase mask that is in contact with a layer of photoresist. These computations use full vector finite element solutions to the problem. (b) Intensity distribution computed for the same system.

wavelengths from the surface of the mask (see Fig. 7) suggest that this technique, which was originally designed for patterning two-dimensional structures of photoresist, may have the capability for generating 3D shapes in thick layers of resists. These and other aspects of the technique are the subject of current work.

Acknowledgements

We thank our collaborators at Harvard University for our initial work with this technique and our collaborators at Bell Labs for the device level applications of it. The recent modeling efforts were performed using funding from the Department of Energy. J.M. acknowledges a fellowship from the government of Portugal.

References

[1] C.A. Mirkin, J.A. Rogers, MRS Bull. 26 (2001) 506.
[2] Y. Xia, J.A. Rogers, K.E. Paul, G.M. Whitesides, Chem. Rev. 99 (1999) 1823–1848.
[3] J.A. Rogers, K.E. Paul, R.J. Jackman, G.M. Whitesides, Appl. Phys. Lett. 70 (1997) 2658–2660.
[4] J.A. Rogers, K.E. Paul, R.J. Jackman, G.M. Whitesides, J. Vac. Sci. Techn. B 16 (1998) 59–68.
[5] J. Aizenberg, J.A. Rogers, K.E. Paul, G.M. Whitesides, Appl. Opt. 37 (1998) 2145–2152.
[6] J.A. Rogers, A. Dodabalapur, Z. Bao, H.E. Katz, Appl. Phys. Lett. 75 (1999) 1010–1012.
[7] J. Aizenberg, J.A. Rogers, K.E. Paul, G.M. Whitesides, Appl. Phys. Lett. 71 (1997) 3773–3775.
[8] T.W. Odom, J.C. Love, D.B. Wolfe, K.E. Paul, G.M. Whitesides, Langmuir 18 (2002) 5314–5320.